International Journal on Magnetic Particle Imaging
Vol 12, No 1, Suppl 1, Article ID 2603015, 3 Pages

Infinite Science Publishing

Proceedings Article

Strong magnetic interaction potentially favors smaller particles in MPS

M. B. Abbas[a,*] · M. Kott[a] · H.-J. Krause[a,b] · U. M. Engelmann[a,*]

[a]Department of Medical Engineering and Applied Mathematics, FH Aachen University of Applied Sciences, 52428 Jülich, Germany
[b]Institute of Biological Information Processing, Forschungszentrum Jülich, Jülich, Germany
*Corresponding author, email: mohamad.abbas@alumni.fh-aachen.de, engelmann@fh-aachen.de

Abstract

Magnetic nanoparticles (MNPs) are pivotal in biomedical applications such as imaging, hyperthermia, and biosensing due to their distinct relaxation dynamics under alternating magnetic fields (AMF). In vivo, MNPs are gradually internalized into cellular and tissue environments, where decreasing interparticle distances – resulting from aggregation, target binding, and dense packing – alter their magnetic response to AMF. These changes amplify magnetic dipole particle-particle interactions (pp-IA) among MNP, notably impacting their relaxation behavior. In this work, we investigate the effect of pp-IA on magnetic particle spectroscopy (MPS) via stochastic simulations coupling Néel and Brownian relaxation mechanisms. Our preliminary results provide evidence that at average interparticle distances below ~50 nm, MNPs with smaller core size (16 nm) yield stronger MPS signals than larger cores (20–28 nm).

I. Introduction

In most medical applications of magnetic nanoparticles (MNP), the MNP will be administered into the bloodstream, where they tend to aggregate at target sites e.g. tumor tissue [1], bind to target biomolecules or become internalized inside cells (e.g. macrophages, dendritic cells) after a certain circulation time [2]. This leads to reduced interparticle distances, r, enlarged hydrodynamic size, d_h, and a more viscous surrounding medium. Recently, we studied the impact of increasing viscosity and enlarged d_h [3] but neglected the impact of interparticle magnetic dipole-dipole interactions (pp-IA) from neighboring MNP, which become more influential for such aggregated MNP. Once below a certain interparticle distance, pp-IA energy dominates thermal activation in neighboring MNP and their pp-IA influences each other's magnetic relaxation behavior [4]. This work is dedicated to systematically study this influence on magnetic particle spectroscopy (MPS) by gradually decreasing interparticle distance for MNP of various core sizes, d_C, assessing its effects on the 3^{rd} harmonics of the resulting MPS signal.

II. Methods and materials

We used stochastic Neel-Brownian coupled relaxation dynamics simulations in python script [5] to predict the magnetic response of magnetite MNP ($M_S = 476 kAm^{-1}$, $K_u = 11 kJ \cdot m^{-3}$, $T = 298K$) to an AMF excitation of $H(t) = H \cdot \sin(2\pi f t)$ with $H = 25 mT/\mu_0$ and $f = 25 kHz$. We assume an excitation field applied in the z-direction (arbitrarily chosen) as well as uniaxial anisotropy. We simulated the dynamic M(H) curves for core sizes of $d_C = (16, 20, 24, 28)$ nm with monodisperse log-normal size distribution width $\sigma = 0.05$, each with hydrodynamic sizes of $d_h = d_C + 10$ nm, modelling e.g. commercial

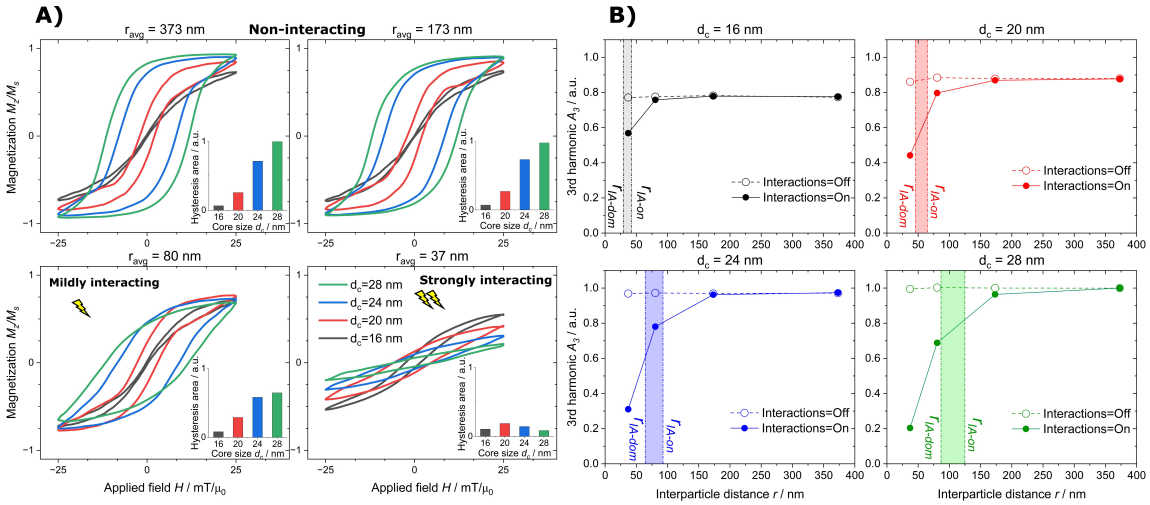

Figure 1: A) Simulated (M-H)-curves for different average interparticle distances r_{avg} for all core sizes d_c with constant hydrodynamic sizes of $d_h = d_c + 10$ nm. Insets show hysteresis area. B) Simulated signal intensity of third harmonic A_3 for different core sizes of increasing pp-IA as r_{avg} decreases (solid lines / full circles) compared to pp-IA turned off (dashed lines / hollow circles). Shaded regions depict the distances marking onset to domination in pp-IA (r_{IA-on} and r_{IA-dom}) for each core size.

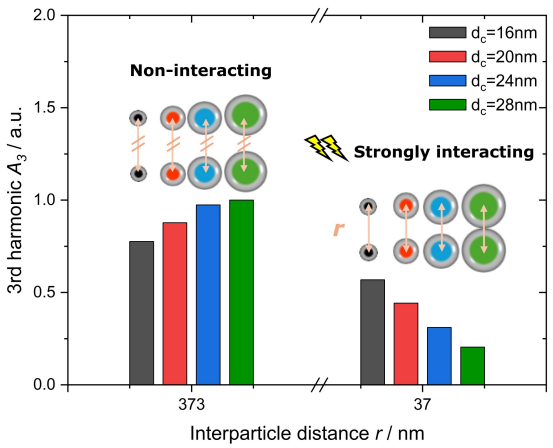

Figure 2: Simulated MPS-signal intensity of third harmonic A_3 dependent on core sizes for non- vs. strongly interacting cases.

Ocean NanoTech particles. Dipolar interaction energy depends on individual interparticle distance r_i by [4]

$$\epsilon_{IA} = \sum_i \frac{\mu_0}{4\pi r_i^3} \cdot \left(\frac{3 \cdot (\mathbf{m}_0 \cdot \mathbf{r}_i) \cdot (\mathbf{m}_i \cdot \mathbf{r}_i)}{\mathbf{r}_i^2} - \mathbf{m}_0 \mathbf{m}_i \right) \quad (1)$$

with MNP individual magnetic moments $|\mathbf{m}_0| = |\mathbf{m}_i| = V_{C,i} \cdot M_S \xrightarrow{r_{avg}} |\hat{m}|$. We suggest that pp-IA become relevant when ϵ_{IA} dominates thermal energy, $\epsilon_{therm} = K_B T$, translating to a range of average interparticle distances, r_{avg}, between the onset of pp-IA at r_{IA-on}, with $\epsilon^{min}_{pp-IA}(r_{IA-on}) \approx \frac{(|\hat{m}|)^2 \cdot \mu_0}{4\pi \cdot r^3_{min}}$ and their full domination at r_{IA-dom} with $\epsilon^{max}_{pp-IA}(r_{IA-dom}) \approx 3 \cdot \frac{(|\hat{m}|)^2 \cdot \mu_0}{4\pi \cdot r^3_{max}}$ [4]. To test our suggestion we probed interparticle distances of $r_{avg} =$ (373, 173, 80, 37) nm.

III. Results and discussion

The chosen values of r_{avg} deliberately expand well outside $r_{1,2}(= 373, 173\ nm) > r_{IA-on}$, i.e. expecting *no pp-IA*, and well within the region $r_4(= 37\ nm) < r_{IA-dom}$, where $\epsilon_{pp-IA} > \epsilon_{therm}$, thus expecting *strong pp-IA* effects (except for $d_c = 16$ nm). For non-interacting distances $r_{1,2}$, the M-(H)-curves (Figure 1A) show larger loops for larger particles, while the M(H)-loop shrinks as the interparticle distance decreases and pp-IA increasingly dominate. Notably, the shrinkage is most prominent for large particles $d_C = 28$ nm, as is evident from the M(H)-enclosed area (s. Figure 1A, insets), while for $d_C = 16$ nm the area of the M(H)-loop increases slightly upon strong pp-IA. The evolution of the third harmonic A_3 with decreasing r_{avg} is shown in Figure 1B: A_3-signal is strongest, where interactions are negligible [6]. However, when interactions are becoming increasingly dominant, the A_3-signal drops substantially. This drop happens sequentially with d_C, affecting large particles first, i.e.: it starts dropping first for core size 28 nm at $r_{avg} = 173$ nm, followed by core size 24 nm at $r_{avg} =$ (173-80) nm, 22 nm at $r_{avg} =$ 80 nm, and lastly 16 nm at $r_{avg} \approx$ (80-37) nm. In general, for all core sizes the A_3-signal drop begins at $r_{avg} > r_{IA-on}$. As expected, strongest MPS-signal (A_3-signal) is generated by largest d_C (= 24, 28 nm) values for non-interacting particles [3,6], as seen in Figure 2. However, this trend is completely reversed for strongly interacting particles, where at $r_{avg} = 37$ nm the relatively strongest A_3-signal is generated by smaller MNP with $d_C = 16$ nm.

10.18416/ijmpi.2026.2603015

According to eq. (1), stronger individual MNP magnetic moments $|\boldsymbol{m}_i| = V_{C,i} \cdot M_S$ obviously increase pp-IA and thereby reduce A_3-signal. However, our simulations are limited by fixed interaction distances and unrealistic aggregation modelling under in-vivo conditions as they neither restrict particle mobility, nor account for changes in hydrodynamic dimensions or chain formations, experimentally shown to alter relaxation behavior [7].

IV. Conclusion

Our preliminary results underline the impact of magnetic interactions at small interparticle distances, $r_{avg} <$ 50 nm, where larger core sizes do not necessarily generate the strongest MPS signal. For in-vivo applications, where MNP aggregate and/or get closely packed inside tissue or cells, this could shift the favor towards MNP of smaller core sizes. Moreover, pp-IA are shown to influence MNP already at interparticle distances larger than expected, $r_{avg} > r_{IA-on}$, potentially showcasing a remarkable effect on MPS signal and thus a need for further investigation.

Acknowledgments

The authors state no funding involved but gratefully acknowledge computational resources provided by FH Aachen UAS (FB9).

Author's statement

Authors state no conflict of interest.

Source code used for simulations can be accessed at https://git.fh-aachen.de/ue8792e/mnp-dynamic-relaxation-simulations.

References

[1] I. Slabu, *et al.*, "Modeling of magnetoliposome uptake in human pancreatic tumor cells in vitro", *Nanotechnology*, vol. 30, no.18, p. 184004, 2019, doi: 10.1088/1361-6528/ab033e.

[2] H. Arami, A. Khandhar, D. Liggitt, and K. M. Krishnan, "In vivo delivery, pharmacokinetics, biodistribution and toxicity of iron oxide nanoparticles", *Chemical Society reviews*, vol. 44, no. 23, pp. 8576–8607, 2015, doi: 10.1039/c5cs00541h.

[3] M. B. Abbas, A. M. Pourshahidi, H.-J. Krause, and U. Engelmann, "How MNP respond to dual-frequency magnetic excitation in viscous media", *International Journal on Magnetic Particle Imaging IJMPI*, vol. 11, 2025, doi: 10.18416/IJMPI.2025.2503033.

[4] U. M. Engelmann, A. Shalaby, C. Shasha, K. M. Krishnan, and H.-J. Krause, "Comparative Modeling of Frequency Mixing Measurements of Magnetic Nanoparticles Using Micromagnetic Simulations and Langevin Theory," *Nanomaterials*, vol. 11, no. 5, 2021, doi: 10.3390/nano11051257.

[5] U. M. Engelmann, C. Shasha and I. Slabu, *Magnetic Nanoparticle Relaxation in Biomedical Application, i*n Magnetic Nanoparticles in Human Health and Medicine: Current Medical Applications and Alternative Therapy of Cancer, 1st ed., C. Caizer, Ed. Hoboken, John Wiley & Sons, 2021, pp. 327–354, doi: 10.1002/9781119754725.ch15.

[6] H.-J. Krause and U. M. Engelmann, "Fundamentals and Applications of Dual-Frequency Magnetic Particle Spectroscopy: Review for Biomedicine and Materials Characterization", *Advanced Science*, vol. 12, no. 13, pp. 2416838, 2025, doi: 10.1002/advs.202416838.

[7] S. L. Saville, *et al.*, "The formation of linear aggregates in magnetic hyperthermia: Implications on specific absorption rate and magnetic anisotropy", *Journal of colloid and interface science*, vol. 424, p. 141-151, 2014, doi: 10.1016/j.jcis.2014.03.007.

